

Measures of black hole masses and virial factors with redshifted broad optical emission lines of AGNs

H. T. Liu^{1,3*}, H. C. Feng^{1,2,3} and J. M. Bai^{1,3}

¹Yunnan Observatories, Chinese Academy of Sciences, Kunming, Yunnan 650011, China

²University of Chinese Academy of Sciences, Beijing 100049, China

³Key Laboratory for the Structure and Evolution of Celestial Objects, Chinese Academy of Sciences, Kunming, Yunnan 650011, China

Accepted . Received

ABSTRACT

Based on redshifted broad optical emission lines in active galactic nuclei (AGNs) containing 13 quasars at redshifts of $1.3 < z < 2.4$ and 1 Seyfert galaxy, we measure black hole masses M_{grav} by using gravitational redshifts of broad lines with respect to forbidden narrow line [OIII] λ 5007. The masses M_{grav} are $\sim 10^{10} M_{\odot}$ for 10 out of 13 high- z quasars, $\sim 10^{11} M_{\odot}$ for the rest of quasars, and $\approx 10^8 M_{\odot}$ for Seyfert 1 galaxy Mrk 110. The virial factors f in the reverberation mapping mass estimation are difficult to be determined due to the unclear kinematics and geometry of broad-line regions (BLRs) of AGNs. Based on a new formula, we estimate f by using the gravitationally redshifted broad emission lines for Mrk 110 and 4 quasars. The different f indicates the different geometry and kinematics of BLRs. The He II and I lines have smaller f than do the Balmer lines for Mrk 110. Mrk 110 has the increasing factors f with the increasing of the BLR sizes, and do these five AGNs as well. This increasing trend results from the radiation pressure influence of accretion disc radiation on the BLR clouds. The radiation pressure seems to be more important than thought usually. Method reliability is tested in Mrk 110. These 10–100 billion M_{\odot} black holes at $1.3 < z < 2.4$ could grow up through the Eddington-limit accretion of black holes in the early Universe.

Key words: black hole physics – gravitation – galaxies: active – galaxies: individual: Mrk 110 – quasars: emission lines – quasars: general.

1 INTRODUCTION

Active galactic nuclei (AGNs), such as quasars and Seyfert galaxies, can be powered by the releases of gravitational potential energy of accretion of matter onto supermassive black holes surrounded by accretion discs (Rees et al. 1982; Rees 1984). It is important to measure the central black hole masses of AGNs. The reverberation mapping model shows that the broad emission line variations are driven by the ionizing continuum variations through the photoionization process (e.g. Blandford & McKee 1982; Peterson 1993). The reverberation mapping observations and researches have been carried out for AGNs over the last several decades (e.g. Kaspi & Netzer 1999; Kaspi et al. 2000, 2007; Peterson et al. 2005; Denney et al. 2010; Haas et al. 2011; Pozo Nuñez et al. 2012; Du et al. 2014, 2015; Pei et al. 2014; Wang et al. 2014; Barth et al. 2015; Hu et al. 2015). A review about the reverberation mapping research studies is given in Gaskell (2009, and references therein). Recently,

some reverberation mapping surveys are proposed and carried out, such as the Sloan Digital Sky Survey spectroscopic reverberation mapping project (Shen et al. 2015a,b,c) and the OzDES AGN spectroscopic reverberation mapping project (King et al. 2015). Thus, the reverberation mapping studies will be the most efficient method to estimate the black hole masses of AGNs. However, the virial factor f in the reverberation mapping mass estimation is uncertain due to the unclear kinematics and geometry of broad-line regions (BLRs) in AGNs (Peterson et al. 2004; Woo et al. 2015). The range of uncertainty in f appears to be 4 orders of magnitude (e.g. Woo & Urry 2002). An average $\langle f \rangle \approx 1$ is derived on the basis of black hole mass–stellar velocity dispersion relation ($M_{\bullet} - \sigma_{\star}$ relation) for the low redshift quiescent galaxies and/or reverberation mapped AGNs using the full widths of half maxima (FWHMs) of the Balmer emission lines (Onken et al. 2004; Piotrovich et al. 2015; Woo et al. 2015).

The BLR cloud motions of the reverberation mapped AGNs are believed and/or assumed to be dominated by the gravitational forces of the central supermassive black

* E-mail: htliu@ynao.ac.cn

holes (i.e., virialized motions) (e.g. Krolik et al. 1991; Wandel et al. 1999; Krolik 2001; Barth et al. 2011). Their virialized motions lead to the observed FWHMs of optical broad emission lines, typically thousands of km s^{-1} . The BLRs usually span from hundreds to thousands of gravitational radii from the central black holes for the reverberation mapped AGNs. At the huge distances, the broad emission lines should be overall redshifted gravitationally by the central black holes. Gravitational redshift in the weak field regime establishes pure shifts of spectral features without changing their intrinsic shapes and in the strong field regime produces remarkable distortions of spectral shapes (Müller & Wold 2006). Distortion is a key feature of relativistic spectra with very skewed and asymmetric line profiles (Fabian et al. 1989; Popovic et al. 1995; Tanaka et al. 1995). The iron $K\alpha$ emission lines in the X-ray spectra of AGNs undergo the remarkable profile deformations in the emitting regions very close to the central black holes (e.g. Fabian et al. 2000; Reynolds & Nowak 2003). These effects are important only very close to the black holes. The broad optical emission lines would not undergo these spectral profile deformations because their BLRs are very distant from the central black holes. Nevertheless, the gravitational redshift still exists for these optical broad lines as long as there are the black holes.

Seyfert galaxies and quasars were first identified with broad Balmer lines and forbidden narrow lines [O III] $\lambda\lambda 4959, 5007$ (Seyfert 1943; Schmidt 1963). Forbidden narrow lines are from narrow-line regions (NLRs) with typical line widths of hundreds of km s^{-1} . The BLRs are much closer to the central black holes than the NLRs (e.g. Urry & Padovani 1995). The redshifts of [O III] $\lambda\lambda 4959, 5007$ are usually regarded as the systematic redshifts of AGNs (e.g. McIntosh et al. 1999). Thus, the redshift increments of the broad Balmer lines with respect to the [O III] narrow lines may be the gravitational redshifts (e.g. Zheng & Sulentic 1990). These redshift differences also may be from the inflow clouds towards the central black holes (e.g. McIntosh et al. 1999). Kollatschny (2003a) ruled out that radial inflow or outflow motions are dominant in the BLR of Seyfert 1 galaxy Mrk 110. The $H\beta$ line in Seyfert 1 galaxy Mrk 50 has an origin in a BLR dominated by orbital motion rather than inflow or outflow (Barth et al. 2011). A variability campaign was performed for Mrk 110 with the high signal-to-noise (S/N) ratio spectra using the 9.2-m Hobby-Eberly Telescope (HET) at McDonald Observatory (Kollatschny et al. 2001). Kollatschny (2003b) found the gravitationally redshifted broad emission lines He II, He I, $H\beta$ and $H\alpha$ with respect to the forbidden narrow line [OIII] $\lambda 5007$. A mean mass of $M_{\text{grav}} = 1.4 \times 10^8 M_{\odot}$ was obtained from the gravitational redshifts of these four broad lines. In this paper, we attempt to estimate the black hole masses and the virial factors f with gravitationally redshifted broad emission lines of AGNs, and investigate whether the factors f depend on the BLR sizes.

The structure of this paper is as follows. Section 2 presents the method. Section 3 describes the applications to quasars. Section 4 presents the applications to Mrk 110. Section 5 explains the accretion growth of black hole. Section 6 presents discussion and conclusions. Throughout this paper, we use the standard cosmology with $H_0 =$

$70 \text{ km s}^{-1} \text{ Mpc}^{-1}$, $\Omega_M = 0.3$, and $\Omega_{\Lambda} = 0.7$ (Spergel et al. 2003; Riess et al. 2004).

2 METHOD

The BLRs are distant from the central black holes for the reverberation mapped AGNs. The Schwarzschild metric will be reasonable to describe the space-time around the BLRs. The Kerr metric and the Schwarzschild metric have the identical effect on the gravitational redshift at the distances larger than about one hundred gravitational radii from the black holes (see Fig. 9 in Müller & Wold 2006). The Schwarzschild space-time is

$$\begin{aligned} ds^2 &= -g_{\mu\nu} dx^{\mu} dx^{\nu} \\ &= \left(1 - \frac{2GM_{\bullet}}{c^2 r}\right) c^2 dt^2 - \left(1 - \frac{2GM_{\bullet}}{c^2 r}\right)^{-1} dr^2 \\ &\quad - r^2 d\theta^2 - r^2 \sin^2 \theta d\varphi^2, \end{aligned} \quad (1)$$

where G is the gravitational constant, c is the speed of light, and M_{\bullet} is the mass of black hole. The ratio of the frequency of atomic transition ν_e at the BLR radius r_{BLR} to the frequency ν_o observed at infinite distance is (static cloud)

$$\begin{aligned} \frac{\nu_o}{\nu_e} &= \frac{(-g_{00})_{r_{\text{BLR}}}^{1/2}}{(-g_{00})_{\infty}^{1/2} c} \\ &= \left(1 - \frac{2GM_{\bullet}}{c^2 r_{\text{BLR}}}\right)^{1/2}, \end{aligned} \quad (2)$$

where $(-g_{00})_{\infty} = 1$ at the observer's frame. So, the gravitational redshift is

$$\begin{aligned} z_g &= \frac{\nu_e}{\nu_o} - 1 \\ &= \left(1 - \frac{2GM_{\bullet}}{c^2 r_{\text{BLR}}}\right)^{-1/2} - 1. \end{aligned} \quad (3)$$

The black hole mass M_{\bullet} is

$$M_{\bullet} = \frac{1}{2} G^{-1} c^2 r_{\text{BLR}} [1 - (1 + z_g)^{-2}], \quad (4)$$

and the first order approximation is

$$M_{\bullet} \cong G^{-1} c^2 z_g r_{\text{BLR}}, \quad (5)$$

if $z_g \ll 1$. Equation (5) is used to estimate M_{\bullet} in Kollatschny (2003b) and Zheng & Sulentic (1990).

In general, the gravitational redshift z_g is derived from the redshift differences of the broad emission lines relative to the narrow emission lines. As the narrow lines do not appear in the spectrum containing the broad lines, the redshift differences $\Delta z_{i,j} = z_i - z_j = z_{g,i} - z_{g,j}$ for the broad lines i and j are used to estimate M_{\bullet} . And then we have

$$\begin{aligned} \Delta z_{i,j} &= \left(1 - \frac{2GM_{\bullet}}{c^2 r_{\text{BLR},i}}\right)^{-1/2} - \left(1 - \frac{2GM_{\bullet}}{c^2 r_{\text{BLR},j}}\right)^{-1/2} \\ &\cong \frac{GM_{\bullet}}{c^2} \left(\frac{1}{r_{\text{BLR},i}} - \frac{1}{r_{\text{BLR},j}}\right), \end{aligned} \quad (6)$$

where $r_{\text{BLR}} \gg r_g = GM_{\bullet}/c^2$ (r_g is the gravitational radius), and

$$M_{\bullet} \cong G^{-1} c^2 \Delta z_{i,j} \left(\frac{1}{r_{\text{BLR},i}} - \frac{1}{r_{\text{BLR},j}}\right)^{-1}, \quad (7)$$

where $r_{\text{BLR},i}$ and $r_{\text{BLR},j}$ correspond to the broad lines i and

j , respectively. Black hole mass can be determined based on the virial theorem for the reverberation mapped AGNs:

$$M_{\text{RM}} = f \frac{v_{\text{FWHM}}^2 r_{\text{BLR}}}{G}, \quad (8)$$

where v_{FWHM} is the FWHM of broad emission line (Peterson et al. 2004). If both of the mapping method and the gravitational redshift method measure the mass M_{\bullet} , the mapping mass M_{RM} is equal to the gravitational redshift mass M_{grav} derived from equation (4) for each AGN. Thus, we have the virial factor

$$f = \frac{1}{2} \frac{c^2}{v_{\text{FWHM}}^2} [1 - (1 + z_g)^{-2}]. \quad (9)$$

3 APPLICATIONS TO QUASARS

Twelve quasars at redshifts $1.3 < z < 2.4$ are collected from Carswell et al. (1991), Nishihara et al. (1997), and McIntosh et al. (1999). Their spectra were observed in the infrared bands. These redshifts of broad H β lines are larger than those of forbidden narrow [O III] λ 5007 lines. These [O III] λ 5007 line redshifts are usually regarded as the rest frames of AGNs and of their host galaxies. The lines [O III] λ 4959, 5007 usually emerge together with the broad line H β . The redshift differences of these broad H β lines with respect to those narrow [O III] λ 5007 lines are identified as the gravitational redshifts z_g . These details are listed in Table 1. For the high- z quasars, Kaspi et al. (2007) have carried out, at the Hobby-Eberly Telescope over the past 6 years, rest-frame ultraviolet spectrophotometric monitoring of a sample of six quasars at $z = 2.2$ – 3.2 , with luminosity of $L_{\text{opt}} \sim 10^{46.4}$ – $10^{47.6}$ ergs s $^{-1}$. The ultraviolet broad emission lines Ly α and C IV λ 1549 were mapped in their observations. The Balmer lines usually used in the reverberation mapping are shifted into the infrared bands, and do the 5100 Å optical continua as well. Thus, it is difficult to map the Balmer line BLR sizes.

A secondary technique to estimate r_{BLR} is the well-known radius-luminosity relation between r_{BLR} and $\lambda L_{\lambda}(5100\text{\AA})$ for the Balmer lines (e.g., Kaspi et al. 2000, 2005; Bentz et al. 2009; Denney et al. 2010). This relation is more applicable to the low- z AGNs in the optical bands. Another radius-luminosity relation is between the radius r_{BLR} and the UV luminosity $\lambda L_{\lambda}(1350\text{\AA})$, and Kaspi et al. (2005) obtained for the broad H β line

$$\frac{r_{\text{BLR}}}{10 \text{ ld}} = A \times \left[\frac{\lambda L_{\lambda}(1350\text{\AA})}{10^{44} \text{ ergs s}^{-1}} \right]^B, \quad (10)$$

where $A = 2.26^{+0.17}_{-0.16}$, $B = 0.557 \pm 0.045$, and $\lambda L_{\lambda}(1350\text{\AA})$ is the 1350 Å luminosity at the rest frame of source. The UV relation is applicable to estimate r_{BLR} of the Balmer lines from $\lambda L_{\lambda}(1350\text{\AA})$ for the high- z AGNs. The 1350 Å fluxes are derived from the optical–UV fluxes taken from the NASA/IPAC Extragalactic Database (NED). The luminosity $\lambda L_{\lambda}(1350\text{\AA})$ is calculated as $z([\text{O III}]\lambda 5007)$ is used. These quasars in Table 1 have $10^{45} < \lambda L_{\lambda}(1350\text{\AA}) < 10^{48}$ ergs s $^{-1}$, which in general are in the same luminosity range as the high- z quasars in Kaspi et al. (2007). The details are presented in Table 1. For these high- z quasars in Table 1, equation (10) will be used to estimate r_{BLR} in equation (4).

The gravitational masses of black holes for these quasars are estimated from equation (4), and are listed in column (8) of Table 1. Their gravitational masses are up to $10^{10} M_{\odot}$ for 10 out of 13 quasars, and the rest quasars have masses up to $10^{11} M_{\odot}$. The virial factors f are estimated for 4 quasars with v_{FWHM} (see Table 2). Q1011+250, Q1630+377 and Q1634+706 have $f = 19.4$, 16.2 and 15.9, respectively. These three values are much larger than the average $\langle f \rangle \approx 1$ derived from the low- z quiescent galaxies and/or reverberation mapped AGNs. Q1331+170 has $f = 5.5$, which is larger than $\langle f \rangle \approx 1$. The four values are estimated for the H α lines. This gravitational redshift approach is a terse method to estimate the virial factor f in the mapping mass estimation. If the BLRs have disc-like geometry with an inclination θ , $f = 1/4 \sin^2 \theta$ (McLure & Dunlop 2001). As $f = 1$, $\theta = 30$ degrees. For the H β lines, three quasars have $\theta \approx 7$ degrees, and one quasar has $\theta \approx 12$ degrees (see Table 2). The quasars have $\theta \approx 5$ – 7 degrees for the H α lines (see Table 2). Our results indicate the nearly face-on view of their accretion discs if their BLRs have disc-like geometry.

4 APPLICATIONS TO MRK 110

The gravitational mass equation used in Kollatschny (2003b) is the same as equation (5) in this paper, the first order approximation to equation (4). The masses M_{grav} derived from equation (4) are presented in Table 3, and are consistent with the mean mass of $\log M_{\text{grav}}/M_{\odot} = 8.15 \pm 0.09$ in Kollatschny (2003b). The virial factors f are derived from equation (9) (see Table 3). The helium and hydrogen lines have different f , and then their BLRs are likely different in the kinematics and geometry. The inclination angle θ is ≈ 7 – 10 degrees (see Table 3). Kollatschny (2003a) previously estimated $\theta = 30 \pm 20^\circ$ from line profile variations, and Kollatschny (2003b) derived $\theta = 21 \pm 5^\circ$ from $f = 1/\sin^2 \theta$. Our results confirm the nearly face-on view of the accretion disc in Mrk 110. The helium line BLRs have slightly larger inclinations than do the hydrogen line ones if their BLRs have disc-like geometry.

If the forbidden narrow lines [O III] λ 4959, 5007 are absent in the spectra, equations (4) and (5) are not appropriate to determine M_{grav} . Equation (7) is appropriate to measure M_{grav} for the AGNs with the [O III] λ 4959, 5007 absent spectra. The black hole masses are derived from equation (7) for Mrk 110 based on different broad emission lines (see Table 4). The estimated masses are $\approx 10^8 M_{\odot}$, and are consistent with those derived from equation (4) in the case of the presence of lines [O III] λ 4959, 5007. This implies that equation (7) is appropriate and reliable to estimate M_{grav} for the AGNs with only some broad emission lines. The gravitational redshifts are not always observable due to the observation accuracies, such as the low S/N ratios and/or the low spectrum resolutions, and the possible contamination of the continua from the jets in radio AGNs.

5 ACCRETION GROWTH OF MASS

We have no idea whether the high- z quasars could grow up to 10^{10} – $10^{11} M_{\odot}$ (see Table 1). In the spherical symmetry

Table 1. Emission line redshifts and black hole masses of quasars

QSO (1)	$z(\text{H}\beta)$ (2)	$z([\text{O III}])$ (3)	z_g (4)	Ref (5)	λF_λ (6)	$\lambda L_\lambda(1350\text{\AA})$ (7)	M_{grav} (8)
					$10^{-12} \text{ ergs s}^{-1} \text{ cm}^{-2}$	$10^{46} \text{ ergs s}^{-1}$	$10^{10} M_\odot$
Q1011+250	1.639±0.001	1.635±0.001	0.004±0.0014	1	$\frac{6.45 \pm 0.107}{6.43 \pm 0.107(0.358\mu\text{m})}$	11.36 ± 0.19	7.97 ± 0.83
Q1630+377	1.478±0.001	1.474±0.001	0.004±0.0014	1	$\frac{11.49 \pm 0.121}{11.10 \pm 0.117(0.358\mu\text{m})}$	15.67 ± 0.16	9.55 ± 1.01
Q1634+706	1.342±0.001	1.336±0.001	0.006±0.0014	1	$\frac{11.21 \pm 0.128}{13.10 \pm 0.150(0.231\mu\text{m})}$	11.99 ± 0.14	12.30 ± 1.08
Q1331+170	2.097±0.001	2.095±0.001	0.002±0.0014	2	$\frac{7.45 \pm 0.096}{6.92 \pm 0.089(0.485\mu\text{m})}$	24.11 ± 0.31	6.09 ± 1.04
Q0109+022	2.356±0.001	2.351±0.0002	0.005±0.0010	3	$\frac{2.46 \pm 0.363}{2.43 \pm 0.359(0.462\mu\text{m})}$	10.54 ± 1.56	9.55 ± 0.81
Q0123+257	2.375±0.0006	2.370±0.0002	0.005±0.0006	3	$\frac{0.200 \pm 0.012}{0.280 \pm 0.017(0.231\mu\text{m})}$	0.87 ± 0.05	2.38 ± 0.13
Q0153+744	2.348±0.0004	2.341±0.0002	0.007±0.0004	3	$\frac{0.049 \pm 0.012}{0.069 \pm 0.017(0.231\mu\text{m})}$	0.21 ± 0.05	1.49 ± 0.07
Q0421+019	2.064±0.0006	2.056±0.0002	0.008±0.0006	3	$\frac{0.754 \pm 0.047}{0.962 \pm 0.060(0.231\mu\text{m})}$	2.33 ± 0.15	6.56 ± 0.39
PG1247+267	2.050±0.0002	2.042±0.0002	0.008±0.0003	3	$\frac{14.16 \pm 0.144}{13.70 \pm 0.139(0.439\mu\text{m})}$	43.03 ± 0.44	33.38 ± 2.80
Q1435+638	2.075±0.0008	2.066±0.0002	0.009±0.0008	3	$\frac{4.73 \pm 0.088}{4.37 \pm 0.081(0.485\mu\text{m})}$	14.79 ± 0.28	20.65 ± 1.57
Q1448-232	2.230±0.0004	2.220±0.0002	0.010±0.0004	3	$\frac{0.528 \pm 0.075}{0.724 \pm 0.103(0.231\mu\text{m})}$	1.97 ± 0.28	7.45 ± 0.43
Q1704+710	2.021±0.001	2.010±0.0002	0.011±0.0010	3	$\frac{0.149 \pm 0.014}{0.197 \pm 0.019(0.231\mu\text{m})}$	0.44 ± 0.04	3.53 ± 0.16
Q2310+385	2.186±0.0008	2.181±0.0002	0.005±0.0008	3	$\frac{1.06 \pm 0.029}{1.05 \pm 0.029(0.439\mu\text{m})}$	3.80 ± 0.10	5.40 ± 0.38

Notes: Column 1: source names; Column 2: redshifts of broad emission line H β ; Column 3: redshifts of narrow forbidden emission line [O III] λ 5007; Column 4: $z_g = z(\text{H}\beta) - z([\text{O III}]\lambda 5007)$; Column 5: references to Columns 1–4; Column 6: fluxes. The down value in each row is the one observed at the wavelength denoted by brackets (obtained in NED, <http://ned.ipac.caltech.edu/>), and the up value is a scaled one at 1350 Å in the rest frame of source according to $f_\nu \propto \nu^{-0.5}$ (e.g., Kaspi et al. 2007). Column 7: the 1350 Å luminosity at the rest frame of source; Column 8: the gravitational masses derived from equation (4).

References: (1) Nishihara et al. 1997; (2) Carswell et al. 1991; (3) McIntosh et al. 1999.

Table 2. Virial factors, black hole masses and accretion disc inclinations of quasars

QSO (1)	v_{FWHM} km/s (2)	z_g (3)	Ref (4)	f (5)	θ° (6)	$\log r_{\text{BLR}}(\text{ld})$ (7)	$M_{\text{grav}}/10^{10} M_\odot$ (8)
Q1011+250	H β 4300	0.004±0.0014	1	19.35±1.46	6.53±0.004	3.06±0.03	7.97 ± 0.83
Q1630+377	H β 4700	0.004±0.0014	1	16.21±1.24	7.14±0.005	3.13±0.03	9.55 ± 1.01
Q1634+706	H β 5800	0.006±0.0014	1	15.90±0.80	7.20±0.003	3.07±0.03	12.30 ± 1.08
Q1331+170	H β 5700	0.002±0.0014	2	5.52±0.84	12.29±0.016	3.24±0.03	6.09 ± 1.04
Q1011+250	H α 3700	0.004±0.0014	1	26.15±1.99	5.61±0.004	3.06±0.03	7.97 ± 0.83
Q1630+377	H α 5300	0.006±0.0014	1	19.06±0.96	6.58±0.003	3.13±0.03	14.30 ± 1.28
Q1634+706	H α 3900	0.005±0.0014	1	29.37±1.78	5.29±0.003	3.07±0.03	10.28 ± 0.96
Q1331+170	H α 4600	0.006±0.0014	2	25.29±1.28	5.71±0.003	3.24±0.03	18.17 ± 1.70

Notes: Column 1: source names; Column 2: FWHMs of broad emission line H β ; Column 3: gravitational redshifts of H β lines; Column 4: references to Columns 1–3; Column 5: the virial factors; Column 6: accretion disc inclinations if BLRs have disc-like geometry; Column 7: r_{BLR} estimated from equation (10) and in units of light days (ld). Column 8: M_{grav} estimated from equation (4).

References: (1) Nishihara et al. 1997; (2) Carswell et al. 1991.

Table 4. M_{grav} from broad lines for Mrk 110

Line (1)	He II λ 5876 (2)	H β λ 4861 (3)	H α λ 6563 (4)
He II λ 4686	8.11 $^{+0.09}_{-0.09}$	8.06 $^{+0.06}_{-0.06}$	8.08 $^{+0.06}_{-0.06}$
He I λ 5876		7.88 $^{+0.14}_{-0.16}$	8.01 $^{+0.11}_{-0.11}$
H β λ 4861			8.39 $^{+0.15}_{-0.20}$

Notes: gravitational masses derived from equation (7) and scaled as $\log \frac{M_{\text{grav}}}{M_\odot}$.

accretion of the fully ionized hydrogen, i.e., the Eddington accretion of a black hole with a mass M_\bullet , the luminosity is

$$L_{\text{Edd}} = \frac{4\pi GM_\bullet(m_p + m_e)c}{\sigma_T} \approx \frac{4\pi GM_\bullet m_p c}{\sigma_T} \quad (11)$$

$$\approx 1.26 \times 10^{38} \frac{M_\bullet}{M_\odot} \text{ ergs s}^{-1},$$

where σ_T is the Thomson cross section, m_p is the rest mass of proton, m_e is the rest mass of electron, and $m_p \gg m_e$ is used. A fraction β of accreted material is to increase M_\bullet . The Eddington luminosity $L_{\text{Edd}} = \eta \dot{M}_{\text{Edd}} c^2$, where \dot{M}_{Edd} is the Eddington mass accretion rate, and η is the percent of the rest mass energy of gases converted into radiation. The radiative efficiency η is 0.057 for a Schwarzschild black hole, 0.423 for a maximally rotating black hole with a prograde accretion disc, and 0.037 for a maximally rotating black hole with a retrograde accretion disc. In general, $\eta = 0.1$ is used. Usually, a mass accretion rate \dot{M} will be a fraction of \dot{M}_{Edd} , i.e., $\dot{M} = \lambda \dot{M}_{\text{Edd}}$. The primary black hole accretes at the rate \dot{M} , and its mass M_\bullet will be increased by $dM_\bullet = \beta \dot{M} dt$ within a time interval of dt . Then we have

$$dM_\bullet \approx \frac{\lambda \beta}{\eta} \frac{4\pi G m_p}{\sigma_T c} M_\bullet dt. \quad (12)$$

Table 3. Gravitational masses, virial factors and accretion disc inclinations of Mrk 110

Line	$\frac{\text{FWHM}(\text{rms})}{\text{km s}^{-1}}$	z_g	τ (days)	$\log \frac{M_{\text{grav}}}{M_{\odot}}$	f	θ°
(1)	(2)	(3)	(4)	(5)	(6)	(7)
He II λ 4686	4444 ± 200	0.00180 ± 0.00020	3.9 ± 2	8.09 ± 0.05	8.18 ± 0.26	10.07 ± 0.003
He I λ 5876	2404 ± 100	0.00062 ± 0.00020	10.7 ± 6	8.06 ± 0.06	9.66 ± 0.69	9.26 ± 0.006
H β λ 4861	1515 ± 100	0.00039 ± 0.00017	24.2 ± 4	8.22 ± 0.04	15.33 ± 1.52	7.34 ± 0.006
H α λ 6563	1315 ± 100	0.00025 ± 0.00017	32.3 ± 5	8.14 ± 0.07	12.98 ± 1.98	7.98 ± 0.011

Notes: Column 1: emission line names; Column 2: FWHMs of broad emission lines; Column 3: gravitational redshifts; Column 4: time lags of lines; Column 5: gravitational masses derived from equation (4); Column 6: the virial factors; Column 7: inclinations if BLRs have disc-like geometry.

Integrating the above formula gives

$$\int_{M_{\bullet}(z_0)}^{M_{\bullet}(z)} \frac{dM_{\bullet}}{M_{\bullet}} \cong \frac{\lambda\beta}{\eta} \frac{4\pi Gm_p}{\sigma_{\text{T}}c} \int_{t_0(z_0)}^{t(z)} dt, \quad (13)$$

where $M_{\bullet}(z_0)$ is the initial mass of black hole in the early Universe, $M_{\bullet}(z)$ is the black hole mass at z , $t(z_0)$ is the Universe age at z_0 , and $t(z)$ is the Universe age at z . Finally, we have

$$\ln \frac{M_{\bullet}(z)}{M_{\bullet}(z_0)} \cong \frac{\lambda\beta}{\eta} \frac{4\pi Gm_p}{\sigma_{\text{T}}c} [t(z) - t_0(z_0)], \quad (14)$$

where $4\pi Gm_p/(\sigma_{\text{T}}c) = 2.218 \text{ Gyr}^{-1}$.

Here, $z_0 = 100$ is assumed and $\eta = 0.1$ is used. $\lambda = 1$ corresponds to the Eddington accretion growth of black hole. First, we consider a black hole with $M_{\bullet}(z) = 10^{10} M_{\odot}$ at $z = 2.4$. As $\beta = 0.9$, $M_{\bullet}(z_0) \cong 10^{-13.1} M_{\odot}$. As $\beta = 0.5$, $M_{\bullet}(z_0) \cong 10^{-2.8} M_{\odot}$. These primary black hole masses are much smaller than the solar mass. Thus, the Eddington accretion growth is possible for the black holes with $M_{\bullet}(z) \sim 10^{10} M_{\odot}$ hosted by quasars in Table 1. Second, a black hole with $M_{\bullet}(z) = 10^{11} M_{\odot}$ at $z = 2.1$ is considered. We have $M_{\bullet}(z_0) \cong 10^{-15.5} M_{\odot}$ and $M_{\bullet}(z_0) \cong 10^{-3.7} M_{\odot}$ for $\beta = 0.9$ and $\beta = 0.5$, respectively. These masses of the primary black holes are small enough for the two quasars at $z \approx 2.1$ with $M_{\bullet}(z) \sim 10^{11} M_{\odot}$ (see Table 1). So, it is possible for the quasars to grow through the Eddington accretion up to $M_{\bullet}(z) \sim 10^{10-11} M_{\odot}$. Quasar J0100+2802 at $z = 6.30$ has a black hole mass of ~ 12 billion M_{\odot} (Wu et al. 2015). Then it seems to be more natural for these 10–100 billion M_{\odot} black holes at $1.3 < z < 2.4$. The masses M_{grav} are reliable for the quasars in Table 1.

6 DISCUSSION AND CONCLUSIONS

Müller & Wold (2006) used the Kerr ray tracing simulations to study the gravitational redshifts of Mrk 110. When $r_{\text{BLR}} \gtrsim 100 r_g$, the simulation results for stationary rotating emitters are nearly identical to, within the errors, those for static emitters in the Kerr space-time and the Schwarzschild space-time (see Fig. 9 in Müller & Wold 2006). So, it is reasonable and reliable to estimate M_{grav} and f by using the formulas in section 2. The helium lines have smaller f than do the hydrogen lines for Mrk 110. This indicates the difference between the BLRs of the helium and hydrogen lines. The inclinations of the helium line BLRs are slightly larger than those of the hydrogen line BLRs (see Table 3). These four broad lines He II, He I, H β , and H α have obvious stratification in the BLRs, as predicted by the virial theorem (Kollatschny 2003b), and are from

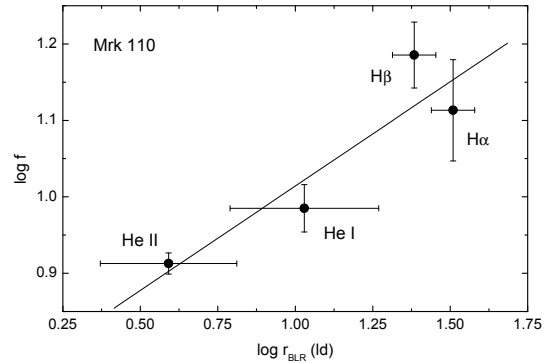


Figure 1. $\log f$ vs $\log r_{\text{BLR}}$ for Mrk 110. The solid line is the best fit with a correlation coefficient $r = 0.91$ at the significance level of 91.4 percent.

the near to the distant away from the central black hole. These stratification BLRs are dominated by the gravity of the central supermassive black hole. In general, the BLR clouds meet the virial theorem for the reverberation mapped AGNs. Mrk 110 will have the virial velocity $v_c^2 = GM_{\bullet} r_{\text{BLR}}^{-1}$ and $v_{\text{FWHM}}^2 \propto v_c^2 \propto r_{\text{BLR}}^{-1}$. We have $f \cong z_g c^2 / v_{\text{FWHM}}^2$ because $z_g \ll 1$ in equation (9) for Mrk 110, and then $f \propto z_g r_{\text{BLR}} \propto M_{\bullet}$ (see equation [5]). M_{\bullet} can be regarded as a constant in observation periods for individual AGNs. So, f is independent of r_{BLR} . However, an increasing trend appears in the plot of $\log f$ versus $\log r_{\text{BLR}}$ for Mrk 110 (see Figure 1). This trend is inconsistent with the independent relation prediction of the virial theorem. We have no idea whether or not this increasing trend is followed by other AGNs. It is tested with both of Mrk 110 and the quasars in Table 2. Except for the H β line of quasar 1331+170, the rest data points basically follow the increasing trend of f with r_{BLR} (see Figure 2).

In the absence of the radiation pressure on the BLR clouds of AGNs with the masses M_{\bullet} , they will have $v_c^2 = GM_{\bullet}/r_{\text{BLR}} = r_{\text{BLR}}^{-1}(r_g) c^2$, where $r_{\text{BLR}}(r_g)$ is in units of r_g . At the same time, $v_{\text{FWHM}}^2 \propto v_c^2 \propto r_{\text{BLR}}^{-1}(r_g)$. Equations (4) and (9) are combined to give $f = GM_{\bullet}/(r_{\text{BLR}} v_{\text{FWHM}}^2) \propto r_{\text{BLR}}^{-1}(r_g)/v_{\text{FWHM}}^2 \propto C$, where C is independent of r_{BLR} and M_{\bullet} . However, Figures 1 and 2 show the evidence of the increasing trend of f with r_{BLR} . So, this problem may result from the ignoring of the radiation pressure on these clouds. The radiation pressure will push these clouds towards the larger radius compared to the BLR radius in the absence of the radiation pressure. Thus, $v_c^2 \neq GM_{\bullet}/r_{\text{BLR}}$ in the presence of the radiation pressure. Thus, we will have $v_{\text{gr}}^2 = GM_{\bullet}/r_{\text{BLR}}/(r_{\text{BLR}}/ld)^{\alpha}$ instead of $v_c^2 = GM_{\bullet}/r_{\text{BLR}}$ for

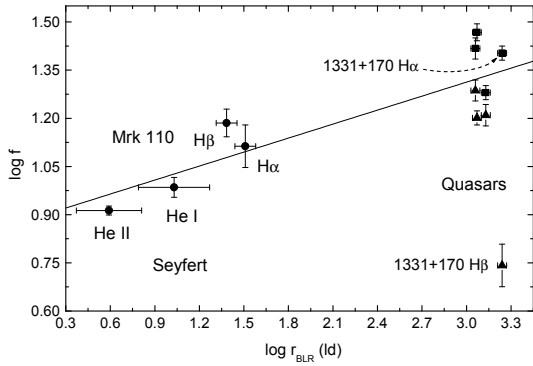


Figure 2. $\log f$ vs $\log r_{\text{BLR}}$ for Mrk 110 and 4 quasars in Table 2. The solid line is the best fit to the data, except for 1331+170 H β data, with a correlation coefficient $r = 0.85$ at the significance level of 99.92 percent. Circles denote Mrk 110, triangles quasars' H β data, and squares quasars' H α data.

the AGNs with luminous accretion discs, where $(r_{\text{BLR}}/l_d)^{-\alpha}$ is the correction factor due to the central disc radiation and $\alpha > 0$. So, $v_{\text{cr}}^2 < v_c^2$ for the same radius r_{BLR} , and $v_{\text{FWHM}}^2 \propto v_{\text{cr}}^2 \propto r_{\text{BLR}}^{-1}(r_g)(r_{\text{BLR}}/l_d)^{-\alpha}$. Thus, $f \propto r_{\text{BLR}}^{-1}(r_g)/v_{\text{FWHM}}^2 \propto (r_{\text{BLR}}/l_d)^\alpha$, i.e., $\log f = D + \alpha \log(r_{\text{BLR}}/l_d)$, where D is independent of r_{BLR} and M_\bullet . The factor f is a function of r_{BLR} rather than $r_{\text{BLR}}(r_g)$, and α is likely different for different AGNs. We have $\alpha \approx 0.27$ for Mrk 110, and $\alpha \approx 0.15$ for the four quasars and Mrk 110 (see Figures 1 and 2). Thus, we confirm that the virial factor f is an increasing function of r_{BLR} , and this increasing trend results from the radiation pressure on these BLR clouds due to the central accretion disc radiation.

Quasar 1331+170 H β data point is apart from the increasing trend of f with r_{BLR} . 1331+170 has a ratio of $z_g(\text{H}\beta)/z_g(\text{H}\alpha) = 1/3$. 1011+250, 1630+377, and 1634+706 have the ratios of 1.0, 2/3, and 1.2, respectively. A mean ratio of 0.96 for the three quasars is distinct from the ratio of 1/3 for 1331+170. Mrk 110 has a ratio of 1.56, which is obviously different from the ratio of 1/3 for 1331+170. These differences challenge the reliability of z_g for the H β line of 1331+170. The H α line of 1331+170 was observed three times on 1987 March 16, 1988 May 1, and 1991 April 21 (Carswell et al. 1991). The three observations give the coherent z_g within the uncertainty of 0.0014 for the H α line. Thus, the z_g of the H α line is more reliable than that of the H β line for 1331+170. So, the data point of the H β line of 1331+170 is excluded in fitting the data in Figure 2. The parameter α in the correction factor of the radiation pressure may be different from one to another AGN. For the individual AGN, the radiation pressure due to accretion disc will produce more obvious effects on the BLR clouds as α increases. As α vanishes, the radiation pressure also vanishes. Mrk 110 has $\alpha \approx 0.27$, and a smaller value of $\alpha \approx 0.15$ is derived from Figure 2 for five AGNs. This smaller value is an averaged result for these five AGNs. All the results of this paper are based on the condition that the optical BLRs are at the distances of hundreds to thousands of r_g away from the central black holes. Mrk 110 has $r_{\text{BLR}} \sim 560\text{--}4100 r_g$ for the lines He II, He I, H β and H α . The quasars in Table 2 have $r_{\text{BLR}} \sim 170\text{--}490 r_g$ for the Balmer lines. So, this

condition is basically met, and the Schwarzschild metric is applicable to describe the space-times around these BLRs.

In this paper, we investigate the black hole mass estimate potential of the redshifted optical broad emission lines in AGNs containing 13 quasars at $1.3 < z < 2.4$ and Seyfert 1 galaxy Mrk 110. The redshifts of broad lines with respect to forbidden narrow line [O III] λ 5007 are regarded as the gravitational redshifts z_g . We derive new formulas and estimate the black hole masses M_{grav} and the virial factors f . The masses M_{grav} are $\approx 10^{10} M_\odot$ for 10 out of 13 quasars, up to $10^{11} M_\odot$ for the rest of quasars, and $\approx 10^8 M_\odot$ for Mrk 110. We estimate f by using z_g and v_{FWHM} of the redshifted broad lines for Mrk 110 and 4 quasars. It is difficult to determine f in the mapping mass estimation due to the unclear kinematics and structures of BLRs in AGNs. The different f implies the different geometry and kinematics of the BLRs. The measurements of f from the redshifted broad lines have the potential to improve the mapping mass estimation. The factors f of these five AGNs are much larger than the mean $\langle f \rangle \approx 1$ derived from the $M_\bullet - \sigma_*$ relation. These estimated factors f increase with the increasing r_{BLR} (see Figures 1 and 2), and this increasing trend results from the radiation pressure of accretion disc radiation in these AGNs. The radiation pressure seems to be more important than thought usually. Approach reliability is tested in Mrk 110 with the high quality observations of reverberation mapping and broad emission line profiles. These 10–100 billion M_\odot black holes at $1.3 < z < 2.4$ will have enough times to grow up through the Eddington limit accretion of black holes in the early Universe, and seem to be more natural because quasar J0100+2802 at $z = 6.30$ has a black hole mass of ~ 12 billion M_\odot . The gravitational masses for these quasars are reliable. The helium lines have smaller f than do the hydrogen lines for Mrk 110, indicating the difference between their BLRs. These five AGNs will have the nearly face-on view of accretion discs if their BLRs have disc-like geometry.

ACKNOWLEDGMENTS

We thank the helpful discussions of Dr. Hui Quan Li. HTL thanks the National Natural Science Foundation of China (NSFC; Grant 11273052) for financial support. JMB acknowledges the support of the NSFC (Grant 11133006). HTL also thanks the financial supports of the project of the Training Programme for the Talents of West Light Foundation, CAS and the Youth Innovation Promotion Association, CAS. This research has made use of the NASA/IPAC Extragalactic Database (NED), which is operated by the Jet Propulsion Laboratory, California Institute of Technology, under contract with the National Aeronautics and Space Administration.

REFERENCES

- Barth A. J. et al., 2011, ApJ, 743, L4
- Barth A. J. et al., 2015, ApJS, 217, 26
- Bentz M. C., Peterson B. M., Netzer H., Pogge R. W., Vestergaard M., 2009, ApJ, 697, 160
- Blandford R. D., McKee C. F., 1982, ApJ, 255, 419

- Carswell R. F. et al., 1991, *ApJ*, 381, L5
 Denney K. D. et al., 2010, *ApJ*, 721, 715
 Du P. et al. (SEAMBH Collaboration), 2014, *ApJ*, 782, 45
 Du P. et al. (SEAMBH Collaboration), 2015, *ApJ*, 806, 22
 Fabian A. C., Rees M. J., Stella L., White N. E., 1989, *MNRAS*, 238, 729
 Fabian A. C., Iwasawa K., Reynolds C. S., Young A. J., 2000, *PASP*, 112, 1145
 Gaskell, C. M. 2009, *NewAR*, 53, 140
 Haas M., Chini R., Ramolla M., Pozo Nuñez, F., Westhues C., Watermann R., Hoffmeister V., Murphy M., 2011, *A&A*, 535, A73
 Hu C. et al. (SEAMBH Collaboration), 2015, *ApJ*, 804, 138
 Kaspi S., Netzer H., 1999, *ApJ*, 524, 71
 Kaspi S., Smith P. S., Netzer H., Maoz D., Jannuzi B. T., Givon U., 2000, *ApJ*, 533, 631
 Kaspi S., Maoz D., Netzer H., Peterson B. M., Vestergaard M., Jannuzi B. T., 2005, *ApJ*, 629, 61
 Kaspi S., Brandt W. N., Maoz D., Netzer H., Schneider D. P., Shemmer O., 2007, *ApJ*, 659, 997
 King A. L. et al., 2015, *MNRAS*, 453, 1701
 Kollatschny W., Bischoff K., Robinson E. L., Welsh W. F., Hill G. J., 2001, *A&A*, 379, 125
 Kollatschny W., 2003a, *A&A*, 407, 461
 Kollatschny W., 2003b, *A&A*, 412, L61
 Krolik J. H., Horne K., Kallman T. R., Malkan M. A., Edelson R. A., Kriss G. A., 1991, *ApJ*, 371, 541
 Krolik J. H., 2001, *ApJ*, 551, 72
 McIntosh D. H., Rix H. W., Rieke M. J., Foltz C. B., 1999, *ApJ*, 517, L73
 McLure R. J., Dunlop J. S., 2001, *MNRAS*, 327, 199
 Müller A., Wold M., 2006, *A&A*, 457, 485
 Nishihara E., Yamashita T., Yoshida M., Watanabe E., Okumura S., Mori A., Iye M., 1997, *ApJ*, 488, L27
 Onken C. A., Ferrarese L., Merritt D., Peterson B. M., Pogge R. W., Vestergaard Ma., Wandel A., 2004, *ApJ*, 615, 645
 Pei L. et al., 2014, *ApJ*, 795, 38
 Peterson B. M., 1993, *PASP*, 105, 247
 Peterson B. M. et al., 2004, *ApJ*, 613, 682
 Peterson B. M. et al., 2005, *ApJ*, 632, 799
 Piotrovich M. Y., Gnedin Yu. N., Silant'ev N. A., Natsvlshvili T. M., Buliga S. D., 2015, *MNRAS*, 454, 1157
 Popovic L. C., Vince I., Atanackovic-Vukmanovic O., Kubicela A., 1995, *A&A*, 293, 309
 Pozo Nuñez, F., Ramolla M., Westhues C., Bruckmann C., Haas M., Chini R., Steenbrugge K., Murphy M., 2012, *A&A*, 545, A84
 Rees M. J., 1984, *ARA&A*, 22, 471
 Rees M. J., Begelman M. C., Blandford R. D., Phinney E. S., 1982, *Nature*, 295, 17
 Reynolds C. S., Nowak M. A., 2003, *Phys. Rep.*, 377, 389
 Riess A. G. et al., 2004, *ApJ*, 607, 665
 Seyfert C. K., 1943, *ApJ*, 97, 28
 Schmidt M., 1963, *Nature*, 197, 1040
 Shen Y., Brandt W. N., Dawson K. S., et al. 2015a, *ApJS*, 216, 4
 Shen Y., Greene J. E., Ho L. C., et al. 2015b, *ApJ*, 805, 96
 Shen, Y. Horne K., Grier C. J. et al. 2015c, arXiv:1510.02802
 Spergel D. N. et al., 2003, *ApJS*, 148, 175
 Tanaka Y. et al., 1995, *Nature*, 375, 659
 Urry C. M., Padovani P., 1995, *PASP*, 107, 803
 Wandel A., Peterson B. M., Makkan M. A., 1999, *ApJ*, 526, 579
 Wang J. M. et al. (SEAMBH Collaboration), 2014, *ApJ*, 793, 108
 Woo J. H., Urry C. M., 2002, *ApJ*, 579, 530
 Woo J. H., Yoon Y., Park S., Park D., Kim S. C., 2015, *ApJ*, 801, 38
 Wu X. B. et al., 2015, *Nature*, 518, 512
 Zheng W., Sulentic J. W., 1990, *ApJ*, 350, 512